Supplemental Figure 1. *Foxp1/4^{DKO}* mutants exhibit AHR. (A) Measurement of lung resistance (rl) in *Foxp1/4^{DKO}* mutants after deducting baseline measurements. (B) Measurement of tissue dampening (g) in *Foxp1/4^{DKO}* mutants after deducting baseline measurements. (C) Measurement of Newtonian resistance (rn) in *Foxp1/4^{DKO}* mutants after deducting baseline measurements (N=6 for control and DKO). (D and E) *Foxp1/4^{DKO}* mutants have a similar level of AHR as control with Af sensitization, and their responses were further amplified after exposed to Af (N = 4). * $P<0.05$.

Supplemental Figure 2. Alterations in immune cell numbers, Npy expression, direct targeting of the Npy promoter by Foxp1/4, and expression of Acta2 and SM22α in Foxp1/4DKO mutants. (A) Loss of Foxp1/4 does not result in any significant increase in eosinophils, macrophages, or lymphocytes but does result in a small increase in neutrophils. This increase in neutrophils also increases the overall cell count numbers in BAL from *Foxp1/4^{DKO}* mutant lungs. (B) Q-PCR data confirming increased Npy expression in *Foxp1/4^{DKO}* mutant lungs. (C) Q-PCR showing epithelial specific increase in Npy expression and enrichment of Scgb1a1 expression in Epcam+ cells from *Foxp1/4^{DKO}* mutant lungs. Acta2 (D and E) and SM22α (F and G) expression was assessed using immunohistochemistry in Scgb1a1cre control and *Foxp1/4^{DKO}* mutants. (H) Acta2 and SM22α was assessed using Q-PCR in Scgb1a1cre and *Foxp1/4^{DKO}* mutants. (I) Location of the two FKH binding sites upstream of the mouse Npy transcriptional start site and their conservation

across species including humans. (J) ChIP assays for Foxp1/4 binding to the Npy -0.8kb enhancer element using Q-PCR. (K) The −0.8kb Npy promoter/enhancer element containing the two FKH binding sites can be repressed by Foxp1 in a dose-dependent manner in a luciferase reporter assay (micrograms of transfected Foxp1 expression plasmid labeled below graph). Scale bar= 50μm, n.s.=not significant.

Supplemental Figure 3. Npy amplifies methacholine-induced bronchoconstriction in mouse airway explants. (A) Mouse PCLS's were treated with 100nM recombinant Npy for 18 hrs, and cumulative dose curves to methacholine measuring luminal diameter narrowing were determined. Line above curve indicates dosages where response was statistically significant. (B) Pretreatment with Npy markedly enhances maximal bronchoconstriction induced by methacholine . **P<0.01.

Supplemental Figure 4. Expression of inflammatory and secretory cell markers in *Foxp1/4^{DKO}:Npy$^{-/-}$* mutants. Expression of IL6 is not significantly changed in either *Foxp1/4^{DKO}* and *Foxp1/4:Npy^{TKO}* mutants compared to Scgb1a1^{cre} controls while expression of KC is increased in and *Foxp1/4:Npy^{TKO}* mutants compared to Scgb1a1^{cre} controls. *P<0.01, **P<0.005.

Supplemental FIgure 5. Expression of Scgb1a1 and Muc5ac in Foxp1/4^{DKO} mutants. Immunostaining was performed on control (A) and *Foxp1/4^{DKO}* mutants (B) for Scgb1a1 and Muc5ac expression. Scale bar=50μm.

Supplemental Figure 6. Expression of *Scgb1a1* in *Foxp1/4^{DKO}* and *Foxp1/4^{DKO}:Npy$^{-/-}$* mutants. Immunohistochemistry for *Scgb1a1* was performed on *Scgb1a1^{cre}* controls (A), *Foxp1/4^{DKO}* (B), and *Foxp1/4:Npy^{TKO}* mutants (C). (D) Q-PCR for *Scgb1a1* expression was performed using whole lung RNA from *Scgb1a1^{cre}* controls, *Foxp1/4^{DKO}*, and *Foxp1/4:Npy^{TKO}* mutants. (E) Expression of goblet cell markers in *Scgb1a1^{cre}* controls, *Foxp1/4^{DKO}*, and *Foxp1/4:Npy^{TKO}* mutants. (F) Expression of Cela2a and Serpin5b in *Scgb1a1^{cre}* controls, *Foxp1/4^{DKO}*, and *Foxp1/4:Npy^{TKO}* mutants. (G) Model of how ectopic/increased Npy expression leads to the AHR phenotype and pre-dispose airways to an asthmatic phenotype. Scale bar=50μm, *P<0.01, **P<0.05.

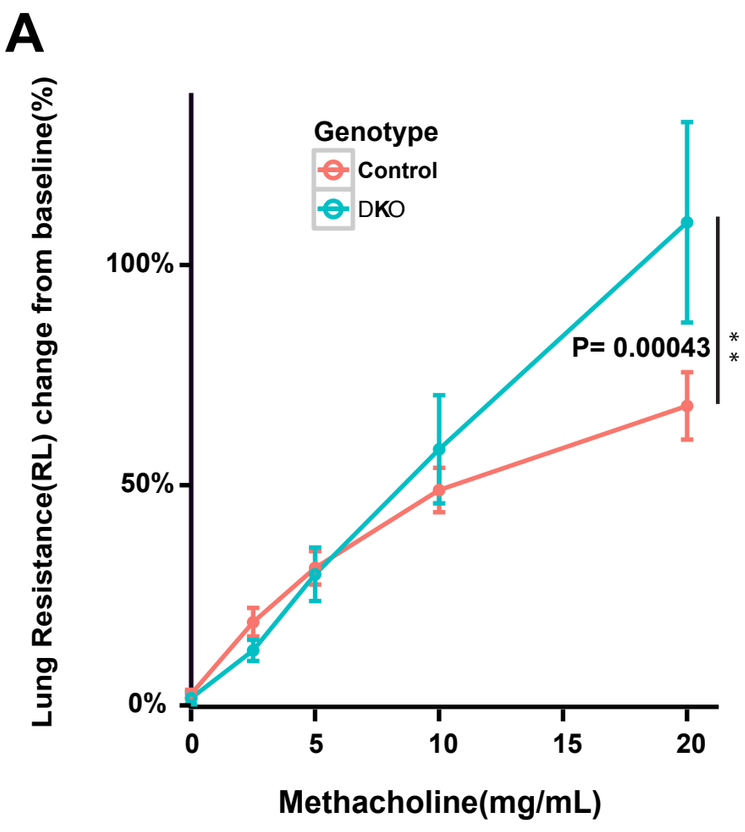

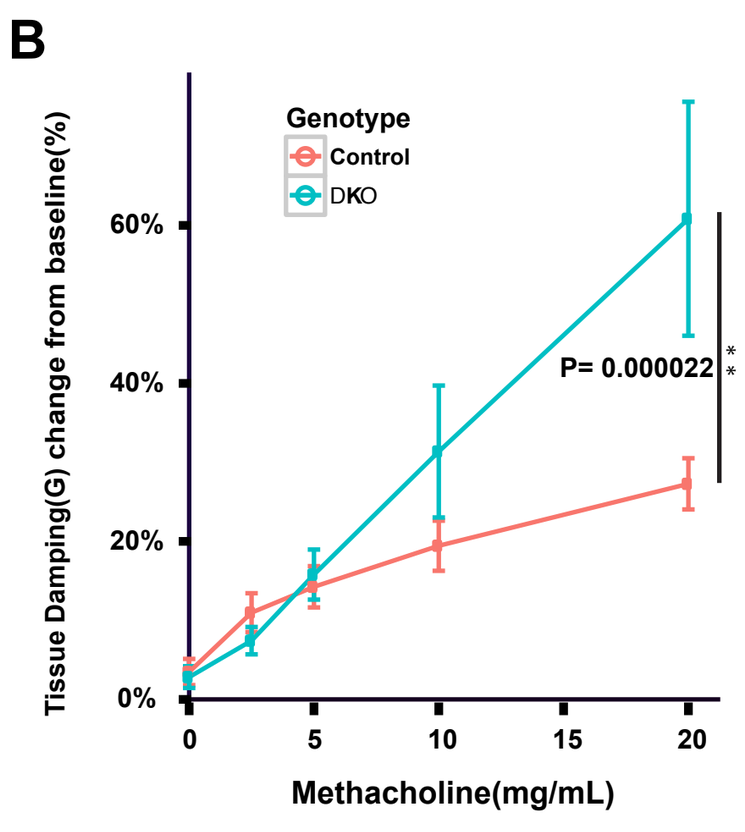

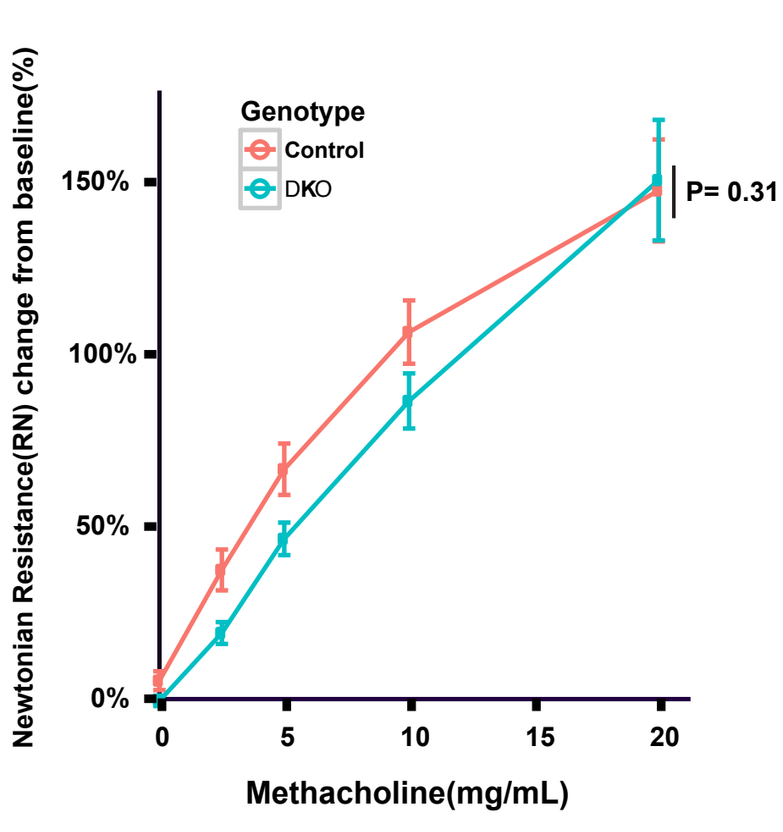

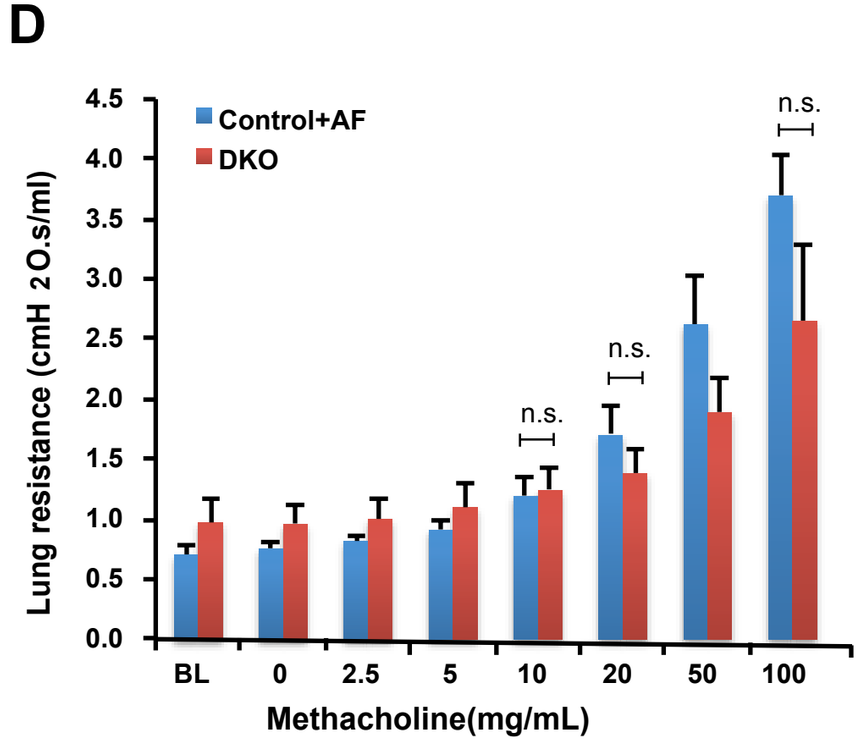

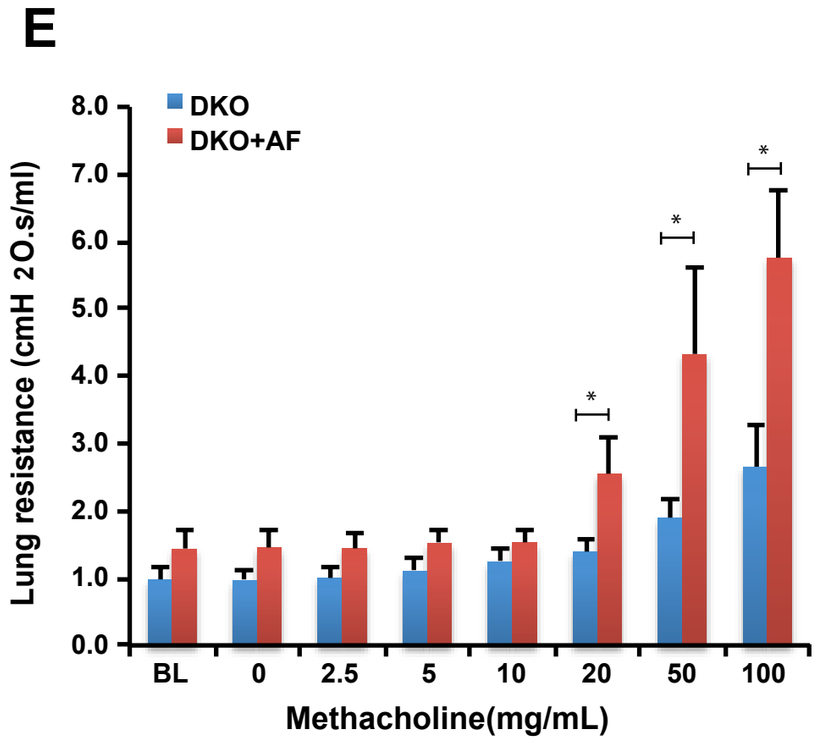

Supplemental Figure 1. Foxp1/4DKO mutants exhibit AHR. (A) Measurement of lung resistance (rl) in Foxp1/4DKO mutants after deducting baseline measurements. (B) Measurement of tissue dampening (g) in Foxp1/4DKO mutants after deducting baseline measurements. (C) Measurement of Newtonian resistance (rn) in Foxp1/4DKO mutants after deducting baseline measurements (N=6 for control and DKO).
(D and E) Foxp1/4DKO mutants have a similar level of AHR as control with Af sensitization, and their responses were further amplified after exposed to Af (N = 4). * P<0.05.

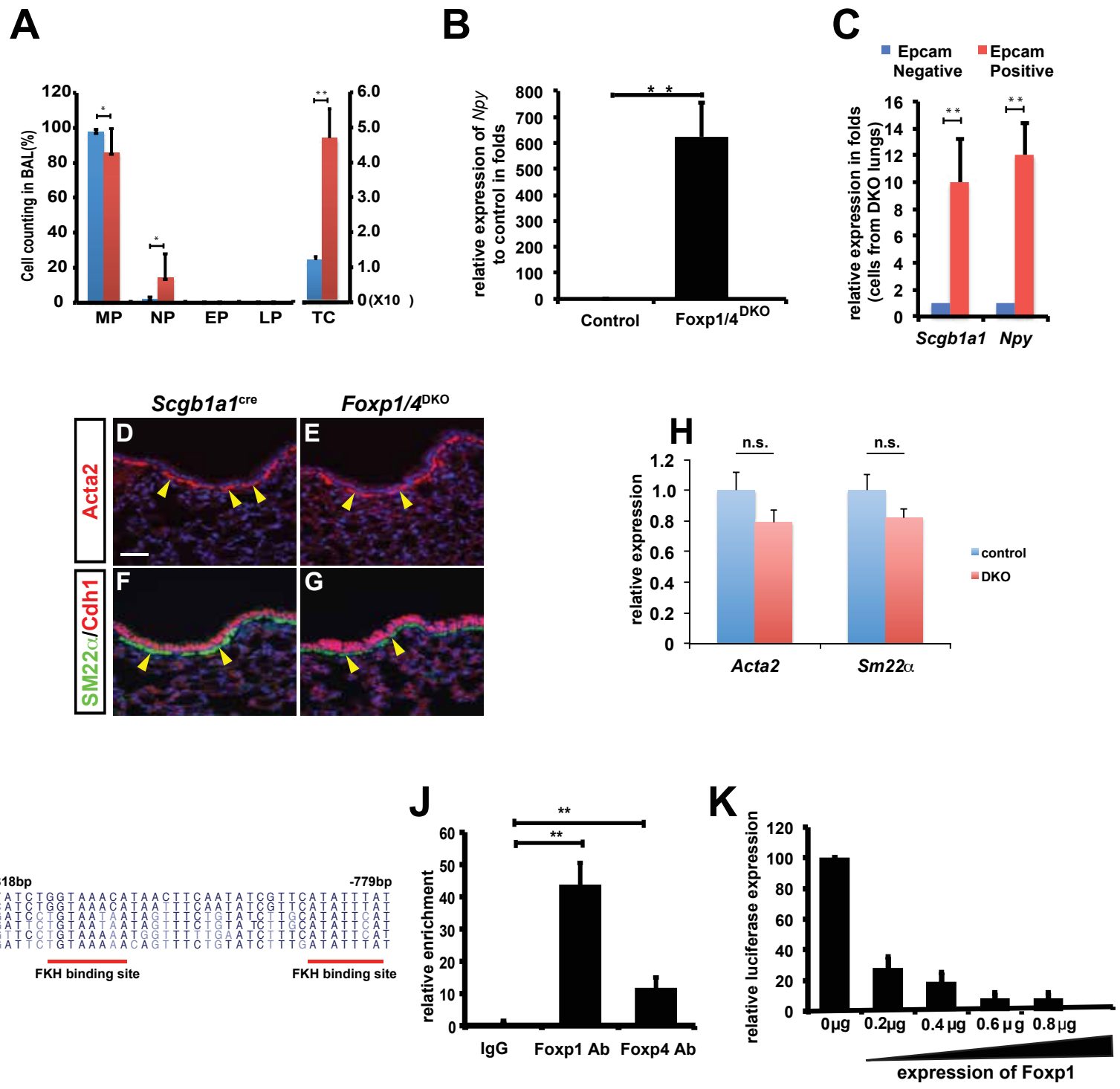

Supplemental Figure 2. Alterations in immune cell numbers, Npy expression, direct targeting of the Npy promoter by Foxp1/4, and expression of Acta2 and SM22α in Foxp1/4^{DKO} mutants. (A) Loss of Foxp1/4 does not result in any significant increase in eosinophils, macrophages, or lymphocytes but does result in a small increase in neutrophils. This increase in neutrophils also increases the overall cell count numbers in BAL from Foxp1/4^{DKO} mutant lungs. (B) Q-PCR data confirming increased Npy expression in Foxp1/4^{DKO} mutant lungs. (C) Q-PCR showing epithelial specific increase in Npy and enrichment of Scgb1a1 expression in Epcam+ cells from Foxp1/4^{DKO} mutant lungs. Acta2 (D and E) and SM22α (F and G) expression was assessed using immunohistochemistry in Scgb1a1cre control and Foxp1/4^{DKO} mutants. (H) Acta2 and SM22α expression was assessed using Q-PCR in Scgb1a1cre and Foxp1/4^{DKO} mutants. (I) Location of the two FKH binding sites upstream of the mouse Npy transcriptional start site and their conservation across species including humans. (J) ChIP assays for Foxp1/4 binding to the Npy -0.8kb enhancer element using Q-PCR. (K) The −0.8kb Npy promoter/enhancer element containing the two FKH binding sites can be repressed by Foxp1 in a dose-dependent manner in a luciferase reporter assay (micrograms of transfected Foxp1 expression plasmid labeled below graph). Scale bar= 50μm, n.s.=not significant.

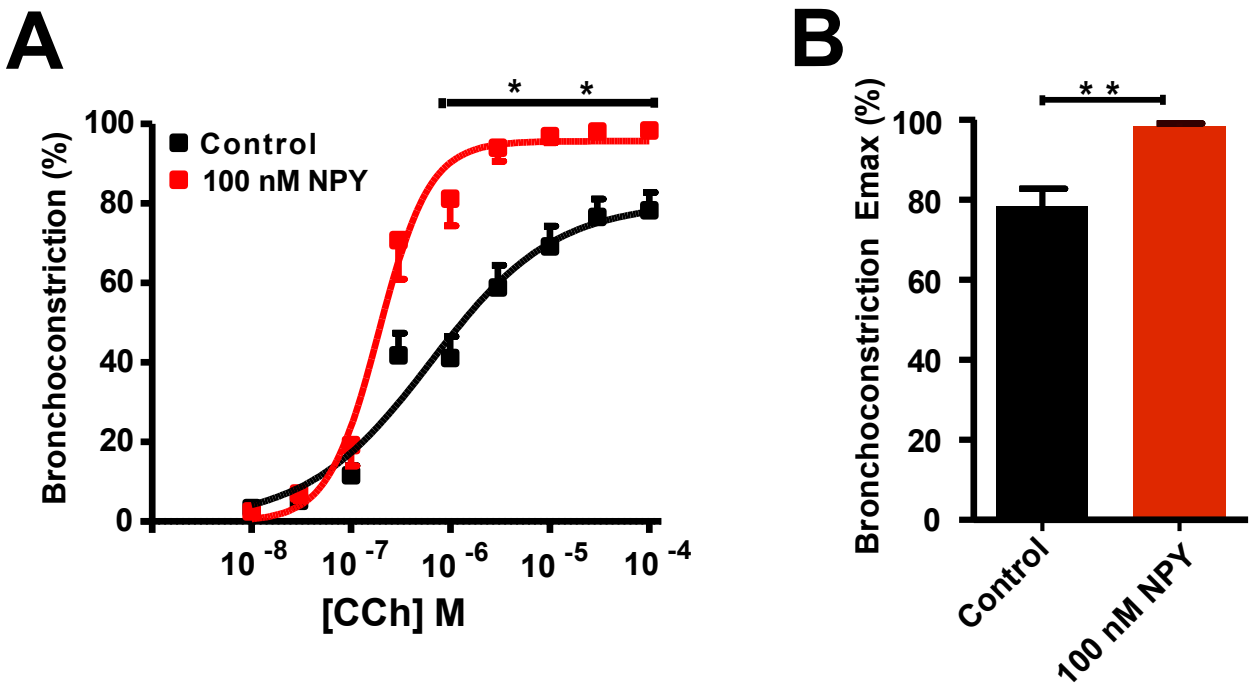

Supplemental Figure 3. Npy amplifies methacholine-induced bronchoconstriction in mouse airway explants. (A) Mouse PCLS's were treated with 100nM recombinant Npy for 18 hrs, and cumulative dose curves to methacholine measuring luminal diameter narrowing were determined. Line above curve indicates dosages where response was statistically significant. (B) Pretreatment with Npy markedly enhances maximal bronchoconstriction induced by methacholine . **P<0.01.

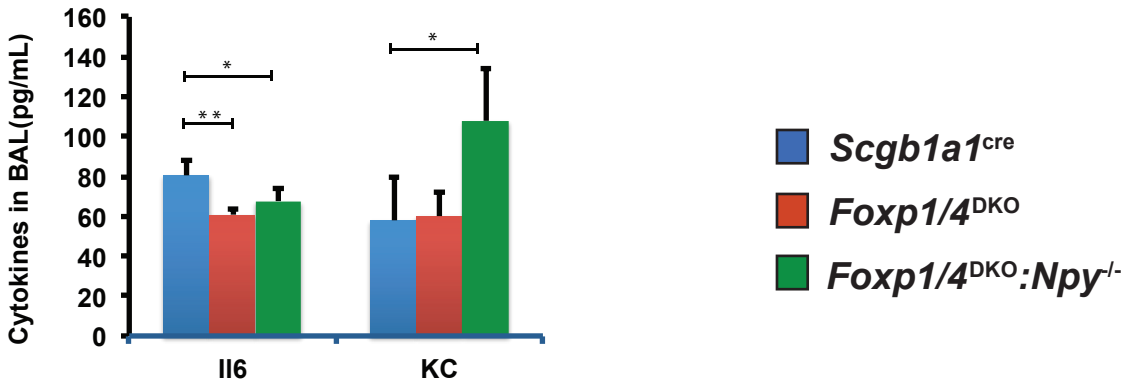

Supplemental Figure 4. Expression of IL6 and KC in Foxp1/4^{DKO} and Foxp1/4:Npy^{TKO} mutant lungs. Expression of IL6 is slightly decreased in both Foxp1/4^{DKO} and Foxp1/4:Npy^{TKO} mutants compared to *Scgb1a1*cre controls while KC is increased in TKO compared to the other two genotypes. *P<0.01, **P<0.005.

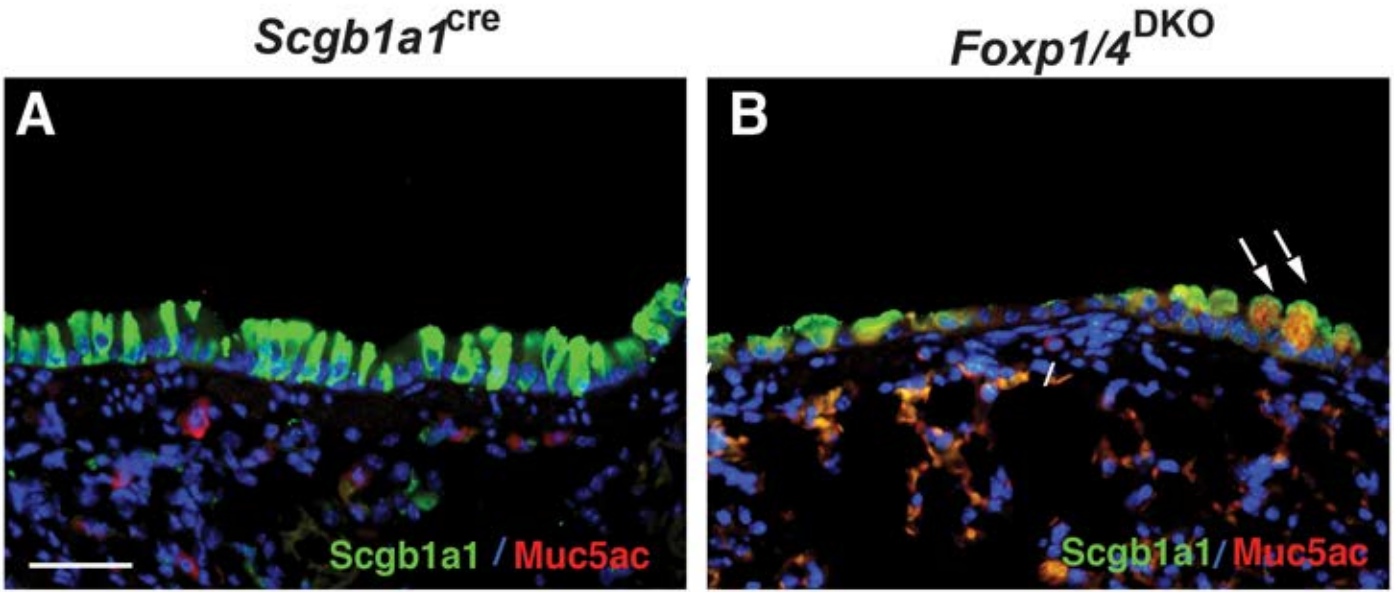

Supplemental FIgure 5. Expression of Scgb1a1 and Muc5ac in Foxp1/4^{DKO} mutants. Immunostaining was performed on control (A) and Foxp1/4^{DKO} mutants (B) for Scgb1a1 and Muc5ac. Scale bar=50μm.

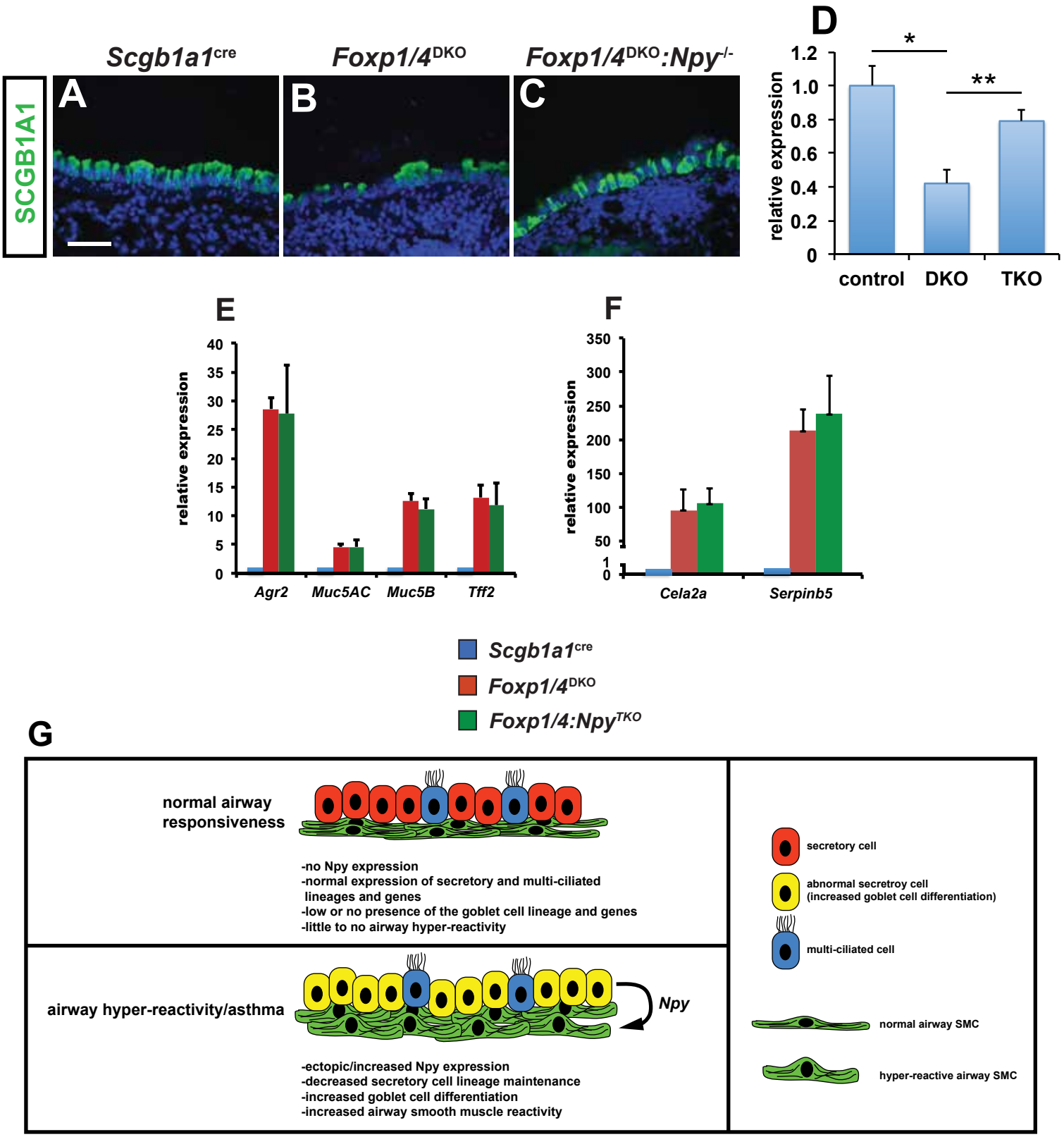

Supplemental Figure 6. Expression of Scgb1a1 and goblet cell markers in *Foxp1/4^{DKO}* and *Foxp1/4:Npy^{TKO}* mutants. Immunohistochemistry for Scgb1a1 was performed on *Scgb1a1^{cre}* controls (A), *Foxp1/4^{DKO}* (B), and *Foxp1/4:Npy^{TKO}* mutants (C). (D) Q-PCR for Scgb1a1 expression was performed using whole lung RNA from *Scgb1a1^{cre}* controls, *Foxp1/4^{DKO}*, and *Foxp1/4:Npy^{TKO}* mutants. (E) Expression of goblet cell markers in *Scgb1a1^{cre}* controls, *Foxp1/4^{DKO}*, and *Foxp1/4:Npy^{TKO}* mutants. (F) Expression of Cela2a and Serpin5b in *Scgb1a1^{cre}* controls, *Foxp1/4^{DKO}*, and *Foxp1/4:Npy^{TKO}* mutants. Scale bar=50μm, *P<0.01, **P<0.05. (G) Model of how ectopic/increased Npy expression leads to the AHR phenotype and pre-dispose airways to an asthmatic phenotype.

Supplemental Materials and Methods

Aspergillus fumigatus (Af)-induced allergic inflammation

The sensitization and challenge with Af was performed as previously described(34). Briefly, 10-12 weeks old female control (*Scgb1a1*^{cre}) (control) and *Foxp1/4*^{DKO} mutant mice were injected intraperitoneally with 20 µg Af combined with 2 mg alum on days 1 and 14, followed by intranasal challenge on Days 25, 26, and 27 with 25 µL of Af extract in PBS (12.5 mg in 21% glycerol, PBS). The total body plethysmography lung function measurement were performed 24 h after their last intranasal treatment.

Lung function measurement

Lung function tests including lung resistance, dynamic compliance, and bronchial alveolar lavage fluid analysis for numbers of leukocytes and concentrations of cytokines were performed as previously described(6). All measurements were generated from at least four 10-12 week old female animals (body weight 18-22g) per time point, agonist concentration, and genotype. Lung resistance (RL), tissue damping (G), Newtonian Resistance (RN) tissue elastance, dynamic compliance, and elastance were recorded using the FlexiVent system (SCIREQ Scientific Respiratory Equipment, Inc., Montreal, PQ, Canada). Airway responsiveness was measured after the inhalation of nebulized saline and increasing concentrations of nebulized Methacholine (0, 2.5, 5, 10, and 20 mg/ml). After measurements, lungs were lavaged with 1 ml aliquots of sterile saline through the tracheal cannula. Differential cell counts identified as

macrophages, eosinophils, neutrophils, and lymphocytes were performed from cytospin preparations. The supernatants were harvested for further analysis. Concentrations of cytokines (IL13, IL17, IL6, KC) in BAL were determined by single analyte ELISA according to standard protocols with recombinant murine cytokines (R&D Systems, Minneapolis, MN) as control samples. Data represent the average of three separate assays each performed in triplicate $\pm$ S.E.M.

Histology

Tissues were collected from all indicated genotype mice between 8-12 weeks of age and were fixed in 10% formalin, embedded in paraffin wax and sectioned at a thickness of 5 μm. Hematoxylin and Eosin (H&E) staining was performed using standard procedures. Immunohistochemistry was performed as previously described using the goat anti-Scgb1a1 (Santa Cruz, 1:20), mouse anti-Muc5ac (Abcam, 1:100), goat anti-SM22α (Abcam, 1:100), rabbit anti-E-cadherin (CDH1) (Cell Signaling, 1:100), mouse anti-Acta2(SMA) (35). Slides were mounted with Vectashield mounting medium containing DAPI (Vector Laboratories). In situ hybridization was performed as previously described(36).

Microarray studies

Differential gene expression performed on the detected gene set between the *Scgb1a1*^{cre} control and *Foxp1/4*^{DKO} mutant mice was analyzed by the Limma package available at the Bioconductor Web site. P-values obtained from the multiple comparison tests were corrected by false discovery rates. Heatmaps

were generated using the R library gplots. Genes with 2-fold or greater changes over that of the experimental mean with a Student's T-test $P<0.01$ (ANOVA) were considered to be statistically significant. RNA was isolated from large proximal airways micro-dissected from adult lungs of *Foxp1/4*^{DKO} and *Scgb1a1*^{cre} control mice and used to determine changes in the transcriptome of airway epithelial cells caused by loss of Foxp1/4 expression. In brief, flash frozen lungs were cut at -20-28^{o}C, and mounted on membrane slides. Slides were fixed in ice-cold 75% EtOH for 2-3min, stained in 1%(w/v in 50% EtOH) cresyl violet (Aldrich) for 2 minutes, washed and dehydrated in ice-cold 70% EtOH, then in 100% EtOH. After air drying for 1-2 min, large proximal airways were micro-dissected into RLT buffer (QIAGENE 74034) using forceps and scissors under a microscope. RNA was isolated and used to generate a biotinylated cRNA probe for Affymetrix Mouse Gene 1.0ST array. Microarray data were analyzed using the Oligo package available at the Bioconductor Web site (http://www.bioconductor.org). The raw data were background-corrected by the robust multichip average (RMA) method and then normalized by an invariant set method.

Quantitative PCR

Total RNA was isolated from lung tissue using QIAGENE Kit (217004), reverse transcribed using SuperScript First Strand Synthesis System (Invitrogen), and used in quantitative real-time PCR analysis with the primers listed in Supplementary Table 1. Data represent the average of three separate assays each performed in triplicate $\pm$ S.E.M.

ChIP analysis

The ChIP assays were performed as previously described (4). The Q-PCR primers are listed in Supplementary Table 1.

Cell culture transfection assays

The *Npy* enhancer containing the two FKH DNA binding sites was cloned into the pGL3 luciferase reporter plasmid to generate pGL3Npy.luc. These were co-transfected into MLE12 cells along with expression plasmid encoding the mouse Foxp1. The luciferase expression assays were performed as previously described(4). Data represent the average of three separate assays each performed in triplicate ± S.E.M.

Lung epithelial cell pull-down assay

Lung epithelia cells were pulled down using EpCAM Antibody (ebioscience 14-5791-85) following the Dynabeads protocol (Invitrogen, 11035). Briefly, adult lungs from *Foxp1/4*^{DKO} mutants were minced and digested into single cells with 3% Collagenase type I(Invitrogen, 17100-017) at 37^{o}C for 30 minutes. After incubated with EpCAM Antibody for 10-15 min at 4^{o}C, single cell suspensions were washed and incubated with pre-washed dynabeads. Both bound(EpCAM enriched) and nonbound (EpCAM nonenriched) cells are collected into RLT buffer (QIAGEN, 74104) for RNA followed by RT-QPCR to examine the expression of Scgb1a1 and Npy.

Protein analysis

Cell lysis and immunoblot analysis were done as previously described(37). Briefly, HASM cells (passage 3-4) were seeded in 6 well or 12 well plates in a completed F12 medium with 10% FBS and antibiotics and grown until confluent. Upon reaching confluence the medium was changed to F12 medium (serum free) for 18-24 hrs with or without NPY treatments (0.1-1μg /ml for 24 hrs), the cells were stimulated with Methacholine (5 μM) for 0 or 10min. Cellular lysates were prepared using RIPA lysis buffer containing 20 mM Tris-HCl (pH 7.5), 150 mM NaCl, 1 mM Na_2EDTA, 1 mM EGTA, 1% NP-40, 1% sodium deoxycholate, 2.5 mM sodium pyrophosphate, 1 mM beta-glycerophosphate, 1 mM Na_3VO_4, and 1 μg/ml leupeptin. Proteins were separated by SDS-PAGE (4–12% Bis-Tris gels) and transferred onto nitrocellulose membranes for Western blotting. Antibodies used to detect pMLC2 (Cell Signaling Technology, #3672) and the loading control β-tubulin (Cell Signaling Technology #3873).

ROCK Activity ELISA

Human airway smooth muscle cells were grown to confluence and serum deprived for 18 hrs. Cells were stimulated with Bradykinin (100 nM) for 10 min. Cellular lysates were prepared using RIPA lysis buffer supplemented with Halt Protease and Phosphatase Inhibitor Cocktail (Thermo Scientific). Protein concentrations were determined using the BCA protein assay kit (Thermo Scientific). ROCK activation was determined using 96-well ROCK Activity Assay

(Cell Biolabs). Data represent the average of three separate assays each performed in triplicate ± S.E.M.

Isolation and culture of primary human airway smooth muscle

HASM cells were derived from tracheas obtained from the National Disease Research Interchange (NDRI) (Philadelphia, PA) and from the International Institute for the Advancement of Medicine (IIAM) (Edison, NJ). HASM cell culture was performed as previously described (6).

Generation of PCLS and bronchoconstriction assays

Mouse and human precision cut lung slices (PCLS) were prepared as previously described (6, 7). Briefly, whole human lungs from donors and mouse lungs were dissected and inflated using 2% (wt/vol) low melting point agarose (37°C) followed by a bolus of air to force the agarose out of the airways and into the parenchymal tissue. Once the agarose set, the largest lobes from mice and the cores (about 8 mm in diameter sectioned from human lungs) were sliced at a thickness of 350 μm(for mouse) or 250 μm (for human) using a Precisionary Instruments tissue slicer (Precisionary Instruments Llc, model VF300). Slices were transferred in sequence to wells containing supplemented Ham's F-12 medium. Suitable airways (≤1-mm diameter) on slices were selected on the basis of the following criteria: presence of a full smooth muscle wall, presence of beating cilia, and unshared muscle walls at airway branch points to eliminate possible counteracting contractile forces. Each slice contained approximately

98% parenchyma tissue; hence, all airways situated on a slice had sufficient parenchymal tissue to impart basal tone. Adjacent slices containing contiguous segments of the same airway were paired and served as controls and were incubated at 37°C in a humidified air/CO_2 (95:5%) incubator. Sections were placed in fresh media every 2-3 hrs during the remainder of *day 1* and all of *day 2* to remove agarose and endogenous substances released that alter airway tone. Slices were incubated overnight (18 hrs) with neuropeptide Y (100nM for mouse, 10nM for human), then bronchoconstricted to a dose response of methacholine (10^{-8} – 10^{-4} M).

To assess luminal area, lung slices were placed in a 12-well plate in media and held in place using a platinum weight with nylon attachments. The airway was located using a microscope connected to a live video feed. Airway luminal area was measured using Image-Pro Plus software (version 6.0; Media Cybernetics) and represented in units of square micrometers. After functional studies, the area of each airway at baseline and at the end of the time course or dose of agonist was calculated using Image-Pro Plus software. A maximum effect (E_{max}) value for each airway was derived from concentration-response curves.